**iScience, Volume *27***

## Supplemental information

# Direct activation of toll-like receptor 4 signaling in group 2 innate lymphoid cells contributes to inflammatory responses of allergic diseases

**Li She, Hamad H. Alanazi, Yimin Xu, Yuxuan Yu, Yuzhang Gao, Shuting Guo, Qingquan Xiong, Hui Jiang, Kexin Mo, Jingwei Wang, Daniel P. Chupp, Hong Zan, Zhenming Xu, Yilun Sun, Na Xiong, Nu Zhang, Zhihai Xie, Weihong Jiang, Xin Zhang, Yong Liu, and Xiao-Dong Li**

# Figure S1

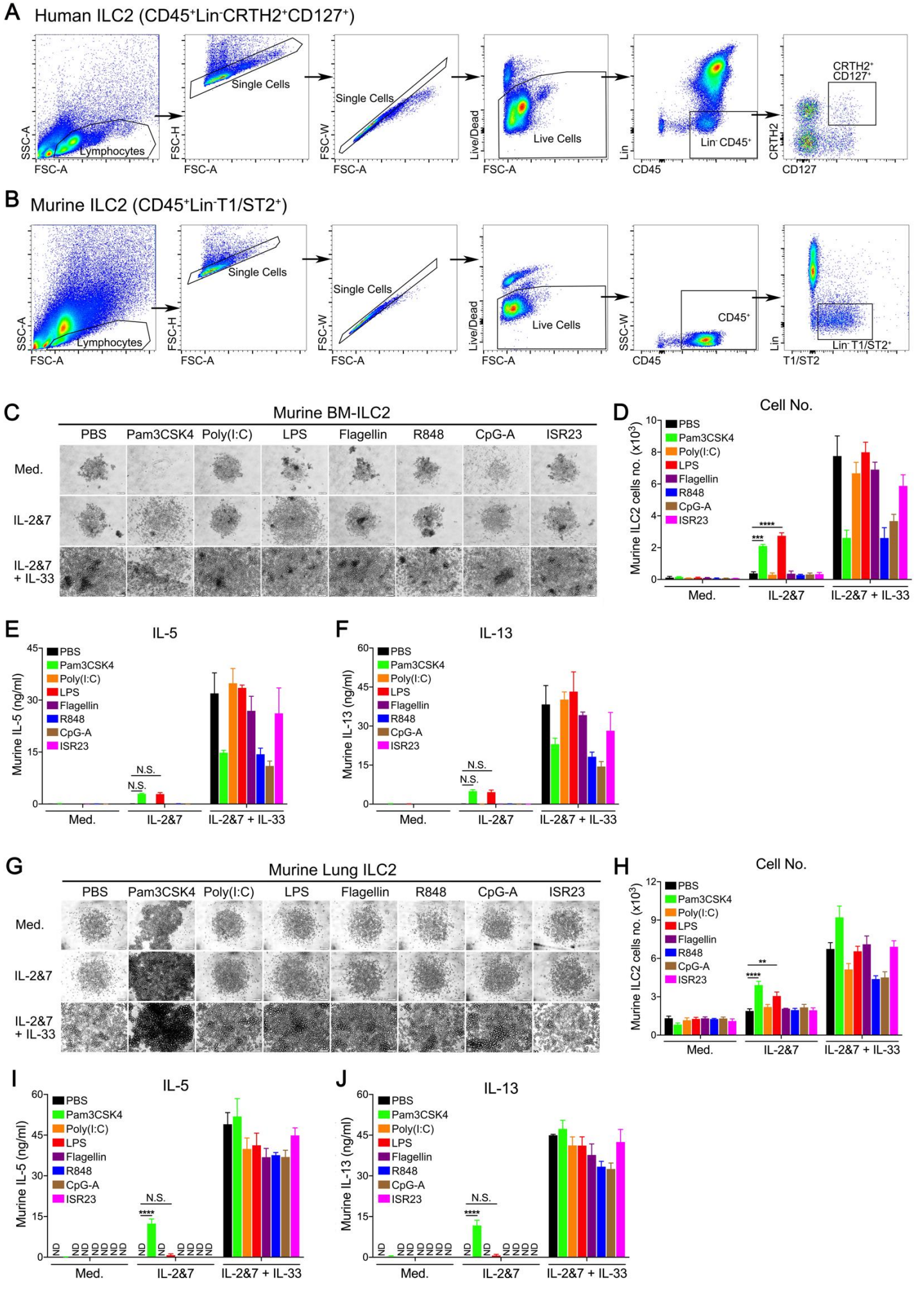
A
Human ILC2 (CD45+Lin-CRTH2+CD127+)
SSC-A
FSC-A
Lymphocytes
FSC-H
Single Cells
FSC-W
Live/Dead
Live Cells
Lin
CD45
Lin- CD45+
CRTH2
CD127
CRTH2+ CD127+
B
Murine ILC2 (CD45+Lin-T1/ST2+)
CD45+
Lin- T1/ST2+
T1/ST2
C
Murine BM-ILC2
PBS
Pam3CSK4
Poly(I:C)
LPS
Flagellin
R848
CpG-A
ISR23
Med.
IL-2&7
IL-2&7 + IL-33
D
Cell No.
Murine ILC2 cells no. (x10³)
N.S.
E
IL-5
Murine IL-5 (ng/ml)
F
IL-13
Murine IL-13 (ng/ml)
G
Murine Lung ILC2
H
I
J
ND

**Figure S1. LPS directly but weakly activated ILC2s from murine lung and bone marrow tissues. Related to Figure 1. A.** Human ILC2s were isolated from the peripheral blood of healthy donors (PBMCs) or umbilical cord blood samples (CBMCs), stained with antibodies against CD45 and lineage markers (CD45+Lin-CRTH2+CD127+), and sorted by the BD FACS Aria. B. Murine lung and bone marrow (BM) ILC2s were isolated from mice treated with recombinant IL-33 protein (250 ng/mouse, intratracheally) and stained with antibodies against CD45 and lineage markers, as described in the Materials and Methods section. Murine ILC2s were sorted by the BD FACS Aria as CD45+Lin-T1/ST2+ cells. The purity of sorted ILC2s was determined to be greater than 95%. C. Light microscopic images showing the growth of murine BM-ILC2s treated with various TLR ligands. Scale bar, 100 μm. D. The number of murine BM-ILC2s from each treatment was quantified by FACS analysis. E. ELISA measuring the production of IL-5 by murine BM-ILC2s treated with various TLR ligands, as indicated. F. ELISA measuring the production of IL-13 by murine BM-ILC2s. G. Light microscopic images showing the growth of murine lung-ILC2s treated with various TLR ligands. Scale bar, 100 μm. H. The number of murine lung-ILC2s from each treatment was quantified by FACS analysis. I. ELISA measuring the production of IL-5 by murine lung-ILC2s treated with various TLR ligands, as indicated. J. ELISA measuring the production of IL-13 by murine lung-ILC2s (two-way ANOVA, **P < 0.01, ***P < 0.001, ****P < 0.0001).

# Figure S2

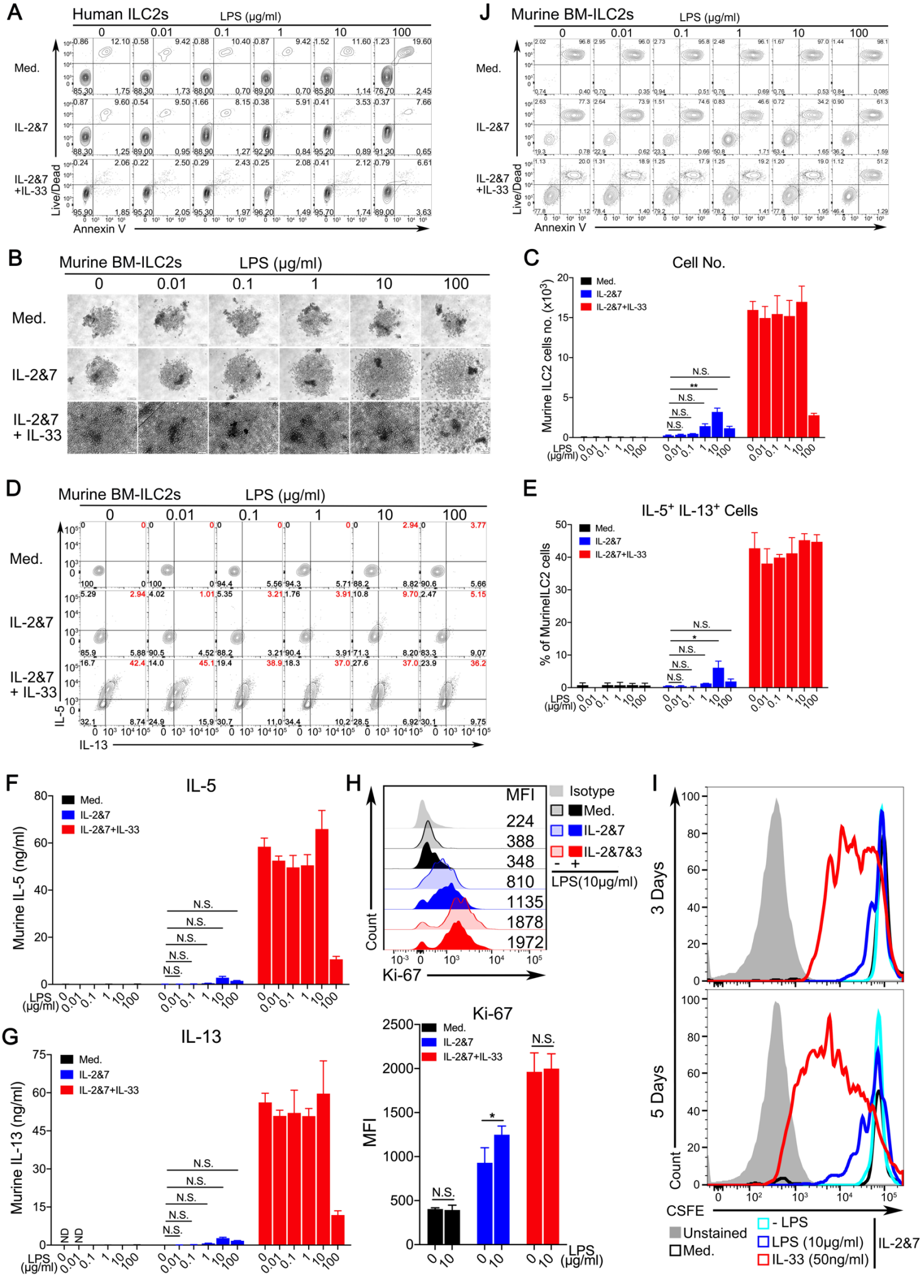
A
Human ILC2s
LPS (μg/ml)
0
0.01
0.1
1
10
100
Med.
IL-2&7
IL-2&7 +IL-33
Live/Dead
Annexin V
J
Murine BM-ILC2s
LPS (μg/ml)
Med.
IL-2&7
IL-2&7 +IL-33
Live/Dead
Annexin V
B
Murine BM-ILC2s
LPS (μg/ml)
Med.
IL-2&7
IL-2&7 + IL-33
C
Cell No.
Murine ILC2 cells no. (x10³)
Med.
IL-2&7
IL-2&7+IL-33
N.S.
**
N.S.
N.S.
N.S.
LPS (μg/ml)
D
Murine BM-ILC2s
LPS (μg/ml)
Med.
IL-2&7
IL-2&7 + IL-33
IL-5
IL-13
E
IL-5⁺ IL-13⁺ Cells
% of MurineILC2 cells
Med.
IL-2&7
IL-2&7+IL-33
N.S.
*
N.S.
N.S.
N.S.
LPS (μg/ml)
F
IL-5
Murine IL-5 (ng/ml)
Med.
IL-2&7
IL-2&7+IL-33
N.S.
N.S.
N.S.
N.S.
N.S.
LPS (μg/ml)
H
MFI
224
388
348
810
1135
1878
1972
Isotype
Med.
IL-2&7
IL-2&7&3
- +
LPS(10μg/ml)
Count
Ki-67
I
3 Days
5 Days
Count
CSFE
Unstained
Med.
- LPS
LPS (10μg/ml)
IL-33 (50ng/ml)
IL-2&7
G
IL-13
Murine IL-13 (ng/ml)
Med.
IL-2&7
IL-2&7+IL-33
ND
ND
N.S.
N.S.
N.S.
N.S.
N.S.
LPS (μg/ml)
Ki-67
MFI
Med.
IL-2&7
IL-2&7+IL-33
N.S.
*
N.S.
LPS (μg/ml)

**Figure S2. LPS weakly stimulated the growth and cytokine production of murine BM-ILC2s. Related to Figure 2. A.** Cell death analysis of human ILC2s on day 3. The cell death of human ILC2s was measured by Live/Dead dye and Annexin V staining using FACS. **B.** Light microscopic images showing the growth of murine BM-ILC2s treated with increasing doses of LPS, as indicated. Scale bar, 100 μm. **C.** The number of murine BM-ILC2s from each LPS dose was quantified by FACS analysis. **D.** The representative FACS result shows the intracellular staining of $IL5^+IL13^+$-double positive murine BM-ILC2s activated by increasing doses of LPS. **E.** The percentage of $IL5^+IL13^+$-double positive murine BM-ILC2s from each LPS dose was quantified by FACS analysis. **F.** ELISA measuring the production of IL-5 (**F**) and IL-13 (**G**) by murine BM-ILC2s treated with increasing doses of LPS. **H.** Representative histogram and summary of the mean fluorescence intensity of murine BM-ILC2s treated with LPS. **I.** CSFE labeling for tracking the proliferation of murine BM-ILC2s treated with LPS or IL-33 for 3 and 5 days. **J.** Cell death analysis of murine BM-ILC2s treated with increasing doses of LPS, as indicated. The cell death was measured by Live/Dead dye and Annexin V staining using FACS (two-way ANOVA, $*P < 0.05$, $**P < 0.01$).

Figure S3

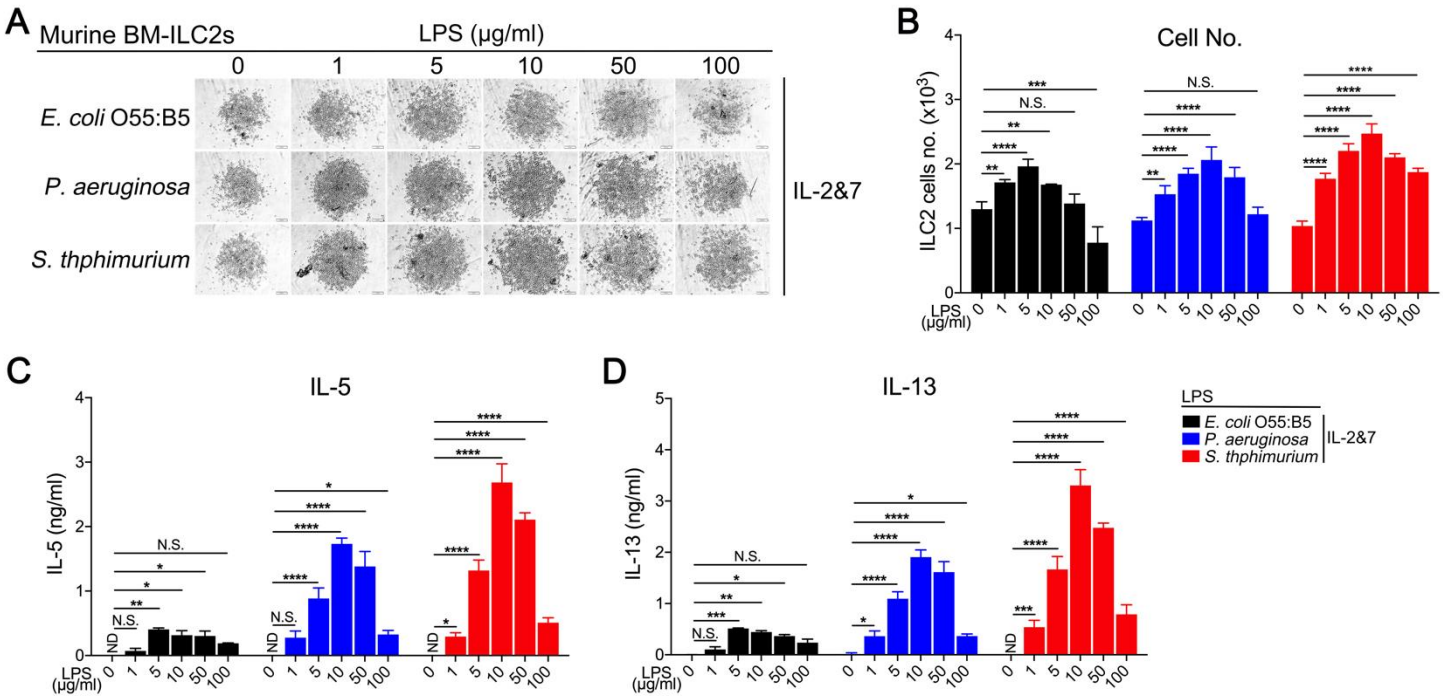


**Figure S3. LPS from various Gram-negative bacterial species could stimulate the growth and cytokine production of murine BM-ILC2s. Related to Figure 2. A.** Light microscopic images showing the growth of murine BM-ILC2s treated with LPS isolated from *E. coli 055:B5*, *P. aeruginosa*, and *S. typhimurium* for 5 days. Each image represented one well in which 1,000 cells were initially seeded. Scale bar, 100 μm. **B.** The number of murine BM-ILC2s treated with different LPS as indicated was quantified by FACS analysis. **C.** ELISA measuring the production of IL-5 by murine BM-ILC2s treated with different LPS as indicated. **D.** ELISA measuring the production of IL-13 by murine BM-ILC2s (two-way ANOVA, **P* < 0.05, ***P* < 0.01, *****P* < 0.0001).

Figure S4

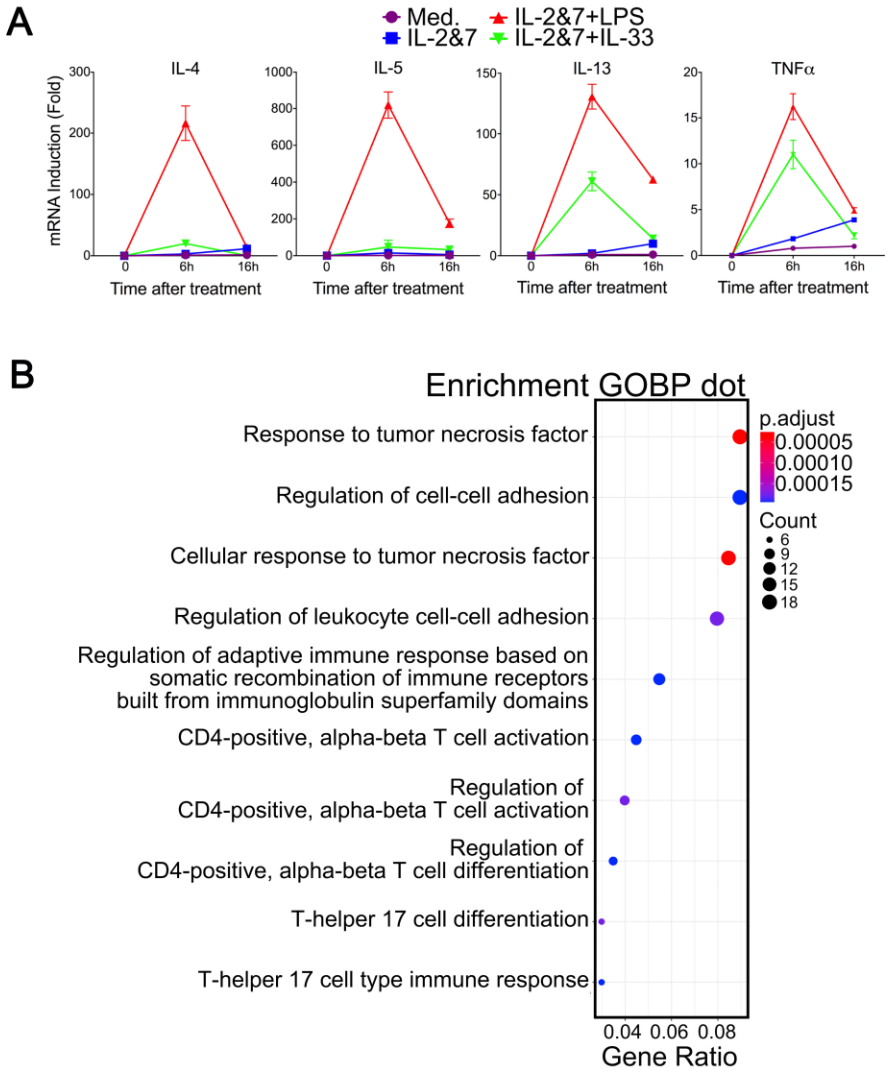


**Figure S4. Gene expression analysis of LPS-stimulated human ILC2s. Related to Figure 4. A.** Human ILC2s were collected followed by RNA isolation at 0, 6, and 16 hours after LPS treatment. The mRNA expression of type 2 cytokines (IL-4, IL-5, and IL-13) and TNFα were measured by RT-qPCR. **B.** Dot plot showing the enrichment analysis of Gene Ontology biological process.

Figure S5

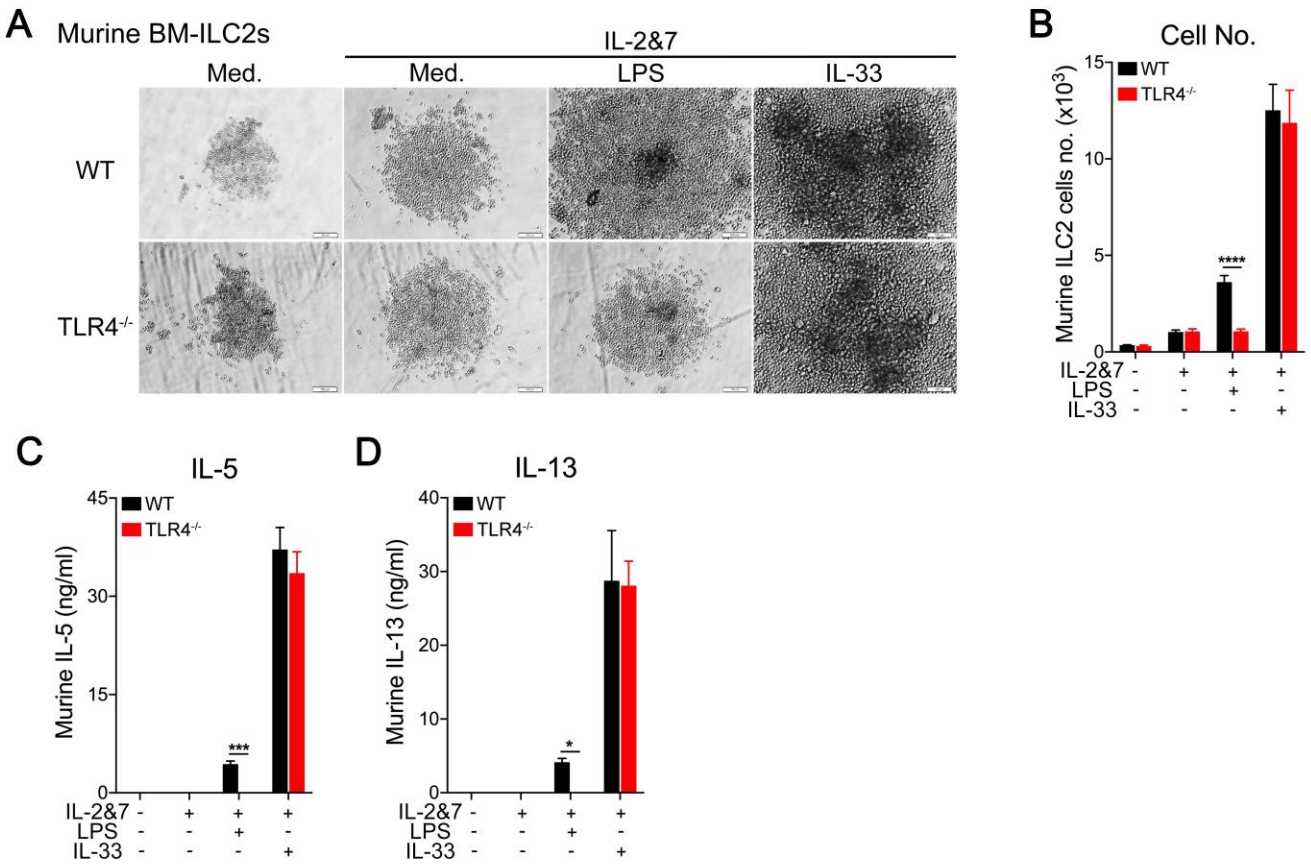


**Figure S5. BM-ILC2s from *TLR4*$^{-/-}$ mouse were unresponsive to LPS stimulation. Related to Figure 5. A.** Light microscopic images showing the growth of murine ILC2s sorted from the bone marrow of WT and *TLR4*$^{-/-}$ mice, were treated with LPS in a 96-well round-bottom plate for 5 days. Each image represented one well in which 1,000 cells were initially seeded. Scale bar, 100 μm. **B.** The number of murine BM-ILC2s after LPS treatment was quantified by FACS analysis. ELISA measuring the production of IL-5 (**C**) and IL-13 (**D**) by murine BM-ILC2s from WT and *TLR4*$^{-/-}$ mice after LPS stimulation. (Unpaired *t*-test, **P* < 0.05, ****P* < 0.001, *****P* < 0.0001).

Figure S6

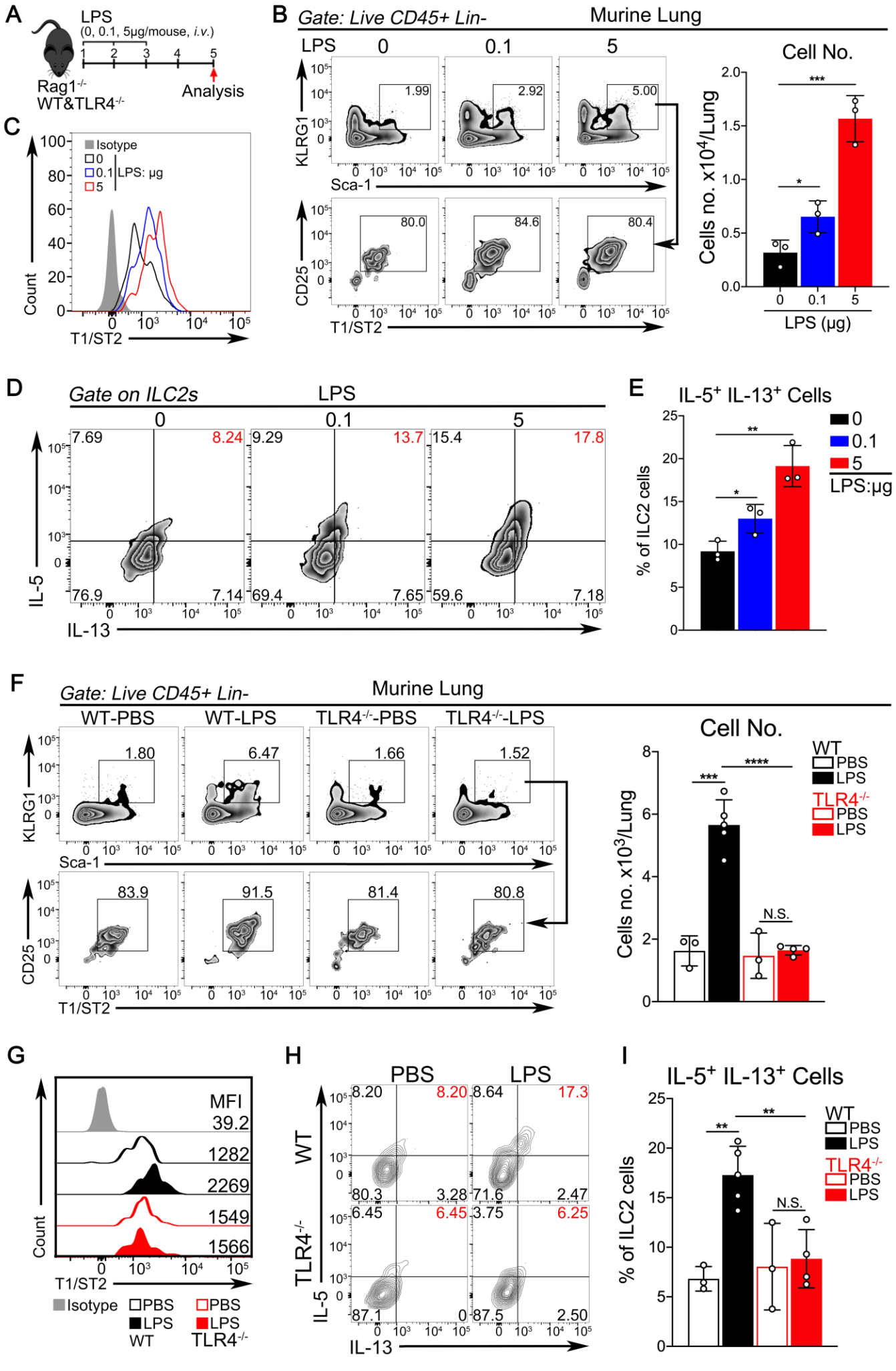
A
LPS
(0, 0.1, 5μg/mouse, i.v.)
1 2 3 4 5
Rag1-/-
WT&TLR4-/-
Analysis
B
Gate: Live CD45+ Lin-
Murine Lung
LPS 0 0.1 5
KLRG1
Sca-1
1.99
2.92
5.00
CD25
T1/ST2
80.0
84.6
80.4
Cell No.
Cells no. x10^4/Lung
LPS (μg)
C
Isotype
0
0.1
5
LPS: μg
Count
T1/ST2
D
Gate on ILC2s
LPS
0 0.1 5
IL-5
IL-13
7.69
8.24
76.9
7.14
9.29
13.7
69.4
7.65
15.4
17.8
59.6
7.18
E
IL-5+ IL-13+ Cells
% of ILC2 cells
LPS:μg
F
Gate: Live CD45+ Lin-
Murine Lung
WT-PBS
WT-LPS
TLR4-/--PBS
TLR4-/--LPS
1.80
6.47
1.66
1.52
83.9
91.5
81.4
80.8
Cell No.
Cells no. x10^3/Lung
WT
PBS
LPS
TLR4-/-
PBS
LPS
N.S.
G
MFI
39.2
1282
2269
1549
1566
Count
T1/ST2
Isotype
PBS
LPS
WT
PBS
LPS
TLR4-/-
H
PBS
LPS
WT
TLR4-/-
IL-5
IL-13
8.20
8.20
80.3
3.28
8.64
17.3
71.6
2.47
6.45
6.45
87.1
0
3.75
6.25
87.5
2.50
I
IL-5+ IL-13+ Cells
% of ILC2 cells
WT
PBS
LPS
TLR4-/-
PBS
LPS
N.S.

**Figure S6. Systemic delivery of LPS into *Rag1*$^{-/-}$ and WT mice, but not *TLR4*$^{-/-}$ mice, triggered the activation of ILC2s *in vivo*. Related to Figure 7. A.** An experimental protocol for studying the activation of murine ILC2s by LPS in a mouse model. **B.** FACS showing the number of murine lung ILC2s in *Rag1*$^{-/-}$ mice, which were intravenously treated with increasing doses of LPS, as indicated. The gating strategy is shown on the left and cell number on the right. **C.** Histogram of ST2 expression levels in murine ILC2s after LPS stimulation. **D.** The percentage of IL5$^{+}$IL13$^{+}$-double positive murine ILC2s in *Rag1*$^{-/-}$ mice was analyzed by intracellular staining. **E.** The percentage of IL5$^{+}$IL13$^{+}$-double positive murine BM-ILC2s was quantified by FACS analysis. **F.** As in **B**, FACS showing the number of murine lung ILC2s in WT and *TLR4*$^{-/-}$ mice, which were intravenously treated with LPS. The gating strategy is shown on the left and cell number on the right. **G.** As in **C**, histogram of ST2 expression levels on murine ILC2s of WT and *TLR4*$^{-/-}$ mice after LPS stimulation. **H.** As in **D**, the percentage of IL5$^{+}$IL13$^{+}$-double positive murine ILC2s in WT and *TLR4*$^{-/-}$ mice was analyzed by intracellular staining. **I.** As in **E**, the percentage of IL5$^{+}$IL13$^{+}$-double positive murine BM-ILC2s in WT and *TLR4*$^{-/-}$ mice was quantified by FACS analysis (unpaired *t*-test, $*P < 0.05$, $**P < 0.01$, $***P < 0.001$, $****P < 0.0001$).

Figure S7

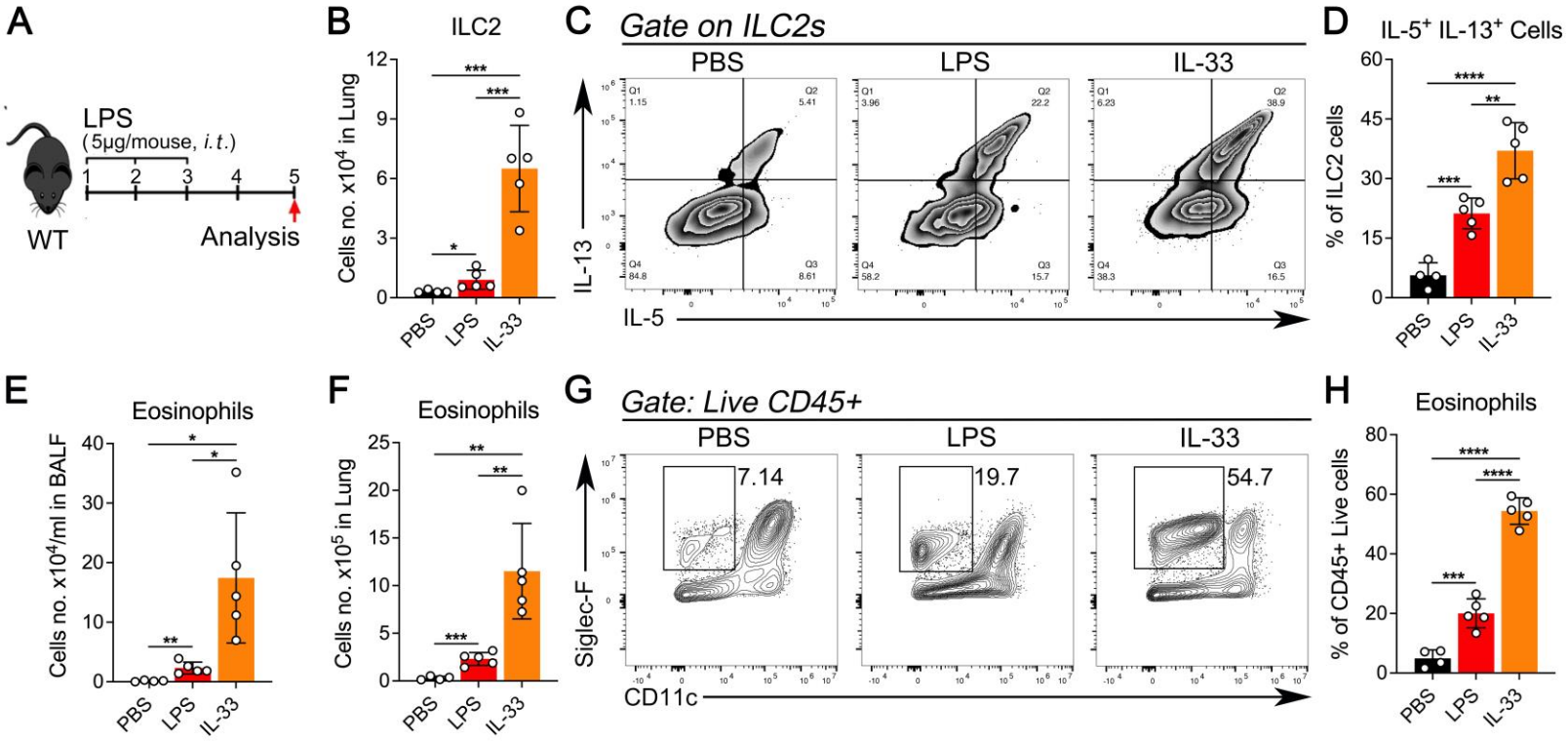


**Figure S7. LPS promoted the activation of ILC2s and eosinophilic airway inflammation *in vivo*. Related to Figure 7. A.** An experimental protocol for studying the activation of murine ILC2s and eosinophilic airway inflammation induced by LPS or IL-33 in a mouse model. **B.** The number of ILC2s in murine lung tissues was quantified by FACS after the mice were treated with LPS or IL-33. **C.** The percentage of IL5$^{+}$IL13$^{+}$-double positive murine ILC2s in the lungs of mice treated with LPS or IL-33 was analyzed by intracellular staining. **D.** The percentage of IL5$^{+}$IL13$^{+}$-double positive murine lung ILC2s was quantified. **E.** The number of eosinophils in the bronchoalveolar lavage fluid (BALF) of mice was determined after treatment with LPS or IL-33 in WT mice. **F.** The number of eosinophils in the lungs of mice treated with LPS or IL-33 was quantified using FACS. **G.** The percentage of eosinophils among CD45$^{+}$ cells in the lungs of mice treated with LPS or IL-33 was analyzed using FACS. **H.** The percentage of eosinophils among CD45$^{+}$ cells was quantified (unpaired *t*-test, **P* < 0.05, ***P* < 0.01, ****P* < 0.001, *****P* < 0.0001).

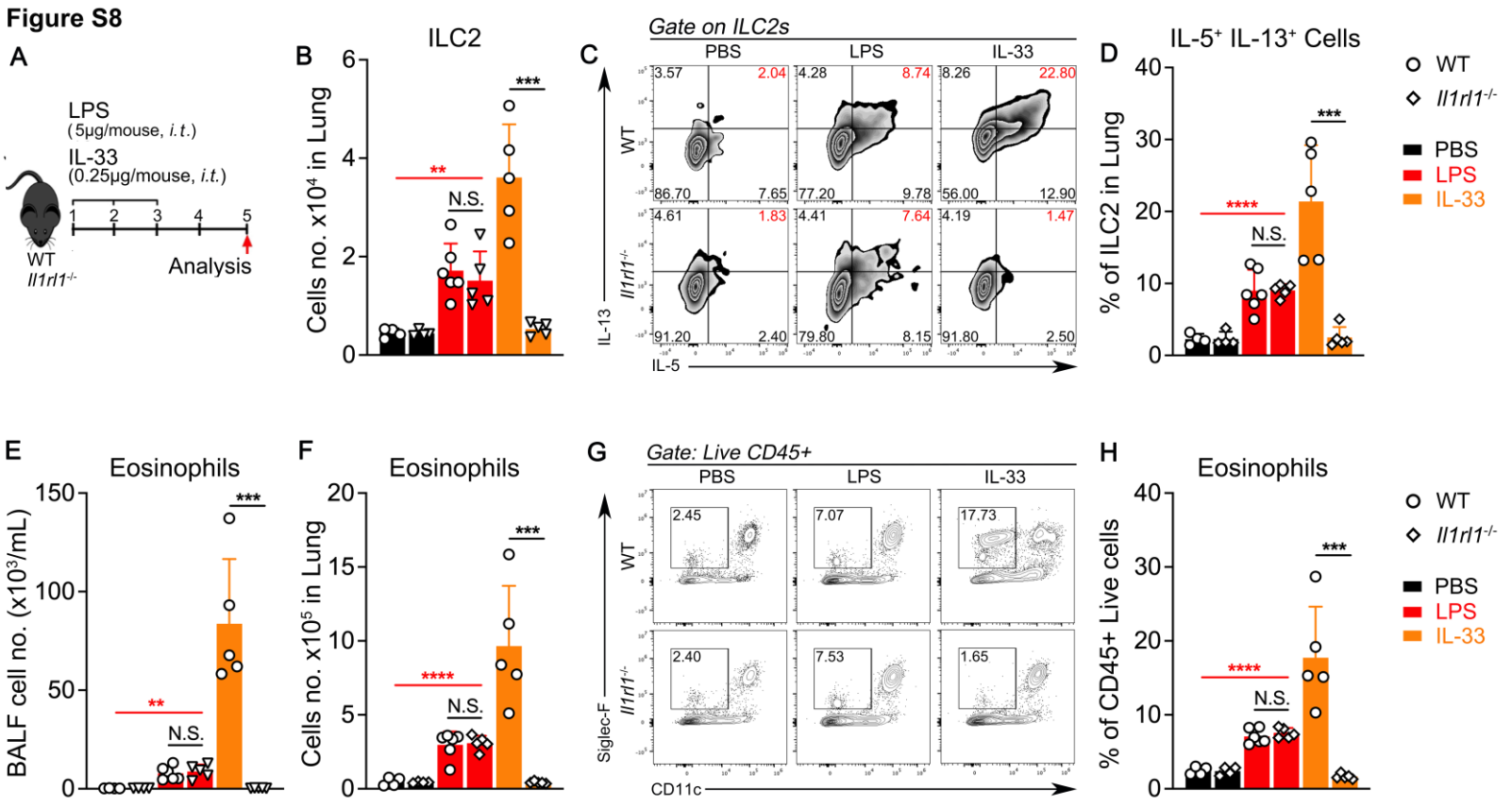


**Figure S8. LPS induces ILC2-mediated eosinophilic inflammation in *Il1rl1*$^{-/-}$ mice. Related to Figure 5. A.** An experimental protocol for studying the activation of murine ILC2s and eosinophilic airway inflammation induced by LPS or IL-33 in WT and *Il1rl1*$^{-/-}$ mice. **B.** The number of ILC2s in murine lung tissues was quantified by FACS after the mice were treated with LPS or IL-33. **C.** The percentage of IL5$^{+}$IL13$^{+}$-double positive murine ILC2s in the lungs of mice treated with LPS or IL-33 was analyzed by intracellular staining. **D.** The percentage of IL5$^{+}$IL13$^{+}$-double positive murine lung ILC2s was quantified. **E.** The number of BALF eosinophils was determined after the treatment with LPS or IL-33 in WT and *Il1rl1*$^{-/-}$ mice. **F.** The number of eosinophils in the lungs of mice treated with LPS or IL-33 was quantified using FACS. **G.** The percentage of eosinophils among CD45$^{+}$ cells in the lungs of mice treated with LPS or IL-33 was analyzed using FACS. **H.** The percentage of eosinophils among CD45$^{+}$ cells was quantified (unpaired *t*-test, $^{**}P < 0.01$, $^{***}P < 0.001$, $^{****}P < 0.0001$).

**Table S1. Clinical information of the patients with allergic rhinitis. Related to Figure 1.**

| No. | Gender | Age | Symptom | | | | | Specific IgE | | PPB* |
|---|---|---|---|---|---|---|---|---|---|---|
| | | | Nasal Obstruction | Rhinocnesmus | Sneeze | Rhinorrhea | Concomitant Symptoms | Dermatophagoides farinae (KUA/L) | Dermatophagoides pteronyssinu (KUA/L) | |
| 1 | F | 23 | N | Y | Y | Y | Eye Itching | 24.40 | 22.80 | NA |
| 2 | M | 9 | Y | Y | Y | Y | None | 35.10 | 48.30 | NA |
| 3 | M | 23 | Y | Y | Y | Y | None | 26.10 | 22.90 | 137 |
| 4 | M | 30 | Y | Y | Y | Y | None | 0.46 | 0.52 | 453 |
| 5 | M | 28 | Y | Y | Y | Y | None | 0.39 | 0.45 | 510 |
| 6 | M | 13 | Y | Y | Y | Y | Eye Itching | 44.30 | 44.90 | NA |
| 7 | F | 16 | Y | Y | Y | Y | None | 5.76 | 4.03 | 257 |
| 8 | F | 23 | Y | Y | Y | Y | None | 10.40 | 15.50 | 412 |
| 9 | M | 13 | Y | Y | Y | Y | None | 63.80 | 49.60 | 466 |
| 10 | M | 16 | Y | Y | Y | Y | None | 0.57 | 0.61 | 460 |
| 11 | F | 20 | Y | Y | Y | Y | Eye Itching | 0.01 | 0.02 | 397 |
| 12 | M | 33 | N | Y | Y | Y | None | 0.17 | 0.20 | 465 |
| 13 | F | 59 | Y | N | Y | Y | None | 0 | 0.03 | NA |
| 14 | M | 12 | Y | N | Y | Y | None | 35.50 | 20.00 | NA |
| 15 | F | 40 | N | Y | Y | Y | None | 15.60 | 21.30 | NA |
| 16 | M | 27 | Y | Y | Y | Y | None | 0.02 | 0.04 | NA |
| 17 | F | 17 | Y | Y | Y | Y | None | 0.67 | 0.61 | NA |
| 18 | F | 16 | Y | Y | Y | Y | Eye Itching | 92.70 | >100 | 234 |
| 19 | M | 42 | Y | Y | Y | Y | Eye Itching | 0.50 | 0.37 | 445 |
| 20 | M | 19 | Y | Y | Y | Y | Eye Itching | 7.51 | 7.20 | 398 |
| 21 | M | 15 | Y | Y | Y | Y | Epistaxis | 0.34 | 0.38 | 364 |
| 22 | M | 12 | Y | Y | Y | Y | Eye Itching | 45.60 | 45.80 | 579 |
| 23 | M | 12 | Y | Y | Y | Y | Eye Itching | 26.30 | 29.20 | 790 |

***PPB: mean fractional exhaled nitric oxide

**Table S2. Clinical information of the patients with atopic dermatitis. Related to Figure 1.**

| No. | Gender | Age | Symptom | Total IgE | Serum IgE (IU/ml) |
|---|---|---|---|---|---|
| 1 | F | 28 | Erythema, Wheal, Pruritus | + | NA |
| 2 | F | 56 | Erythema, Wheal, Pruritus | NA | 100.10 |
| 3 | M | 12 | Erythema, Wheal | + | 534.90 |
| 4 | F | 25 | Wheal, Pruritus | + | 8.50 |
| 5 | F | 14 | Wheal, Pruritus | + | 161.20 |
| 6 | F | 42 | Wheal, Puritus | + | 26.90 |
| 7 | M | 29 | Rash， Wheal | NA | NA |
| 8 | F | 20 | Rash， Wheal | NA | NA |
| 9 | F | 50 | Rash， Wheal | NA | NA |
| 10 | F | 26 | Rash， Wheal | NA | NA |
| 11 | M | 52 | Rash， Wheal | NA | NA |